Journal of the European Ceramic Society **19** (1999) 2437–2447

PII: S0955-2219(99)00127-2
0955-2219/99/$ - see front matter

Layered Perovskites as 'Soft-ceramics'

Geoff Fair,[a†] Michael Shemkunas,[a] William T. Petuskey[a*] and Sankar Sambasivan[b]

[a]Department of Chemistry and Biochemistry and the Science and Engineering of Materials Program, Arizona State University, Tempe, AZ 85287-1604, USA
[b]ACTG, Northwestern University, Evanston, IL 60201-3135, USA

Abstract

The layered perovskite $KCa_2Nb_3O_{10}$ is shown to possess large elastic and fracture anisotropies which are explained on the basis of its structure. Its fracture toughness was measured relative to the in-basal and basal-normal directions. Combined with previously determined elastic moduli, the fracture energy release rates and associated anisotropy were determined and discussed in terms of crack deflection characteristics. The general mechanical characteristics of $KCa_2Nb_3O_{10}$ were discussed relating to what is described as a 'soft' ceramic capable of sustaining considerable mechanical damage. Its high thermal stability, $T_m = 1464°C$, and its oxidation resistance are additional features that make it attractive for high temperature applications. Anecdotal demonstrations of its softness and low damage thresholds are presented, such as might be important for cerarnic–matrix composites or machinable ceramic applications. © *1999 Elsevier Science Ltd. All rights reserved.*

Keywords: anisotropy, $KCa_2Nb_3O_{10}$, niobates, perovskites, toughness.

1 Introduction

The term 'soft-ceramics' is a combination of words that are not often used together, considering that most ceramic applications focus on high hardness, chemical resistance and thermal refractoriness. Nevertheless, new applications are always being sought that rely on unusual combinations of physical and chemical properties. Here, we examine layered perovskites for their mechanical softness keeping in mind that many are also thermally stable in oxidizing and reducing environments up to, typically, between 1450 and 1650°C.

Layered perovskites, such as the Dion–Jacobson phases, are already of great interest because of their characteristics as hosts for intercalation chemistry.[1–3] One compound has been discovered to superconduct at very low temperatures, despite the fact that it is insulating at room temperature.[4] However, we find them interesting because they are intrinsically weak and capable of sustaining considerable damage under low loads, such as might be imposed by microhardness and nanohardness indenters. We recently proposed their use as boundary phases in ceramic–matrix composites,[5] because they behave similarly to the micas, graphite and hexagonal boron nitride in deflecting cracks in ceramic composites. They possess layered crystal structures that cleave very easily along the crystallographic basal planes; and they easily delaminate and exfoliate in the presence of bending and buckling stresses.

In this paper, we discuss some of the physical and chemical characteristics of layered perovskites and provide anecdotal demonstrations of their mechanical applications. We focus on the compound $KCa_2Nb_3O_{10}$ in particular because much information on its preparation, handling and characterization is already provided by research on intercalation chemistry. In a sense, it represents a class of compounds that possesses a moderately broad range of compositions and, therefore, has some prospect for adaptation and design for specific applications.

Experimental results are presented on the fracture toughness of hot pressed $KCa_2Nb_3O_{10}$. Because the material was highly textured, exhibiting strong preferential orientation, measurements were taken on specimens cut from the main stock in three orthogonal directions. The differences are related to the anisotropy of the crystal structure. Combined with previously determined elastic moduli, the anisotropy of the fracture energy release rate is examined in the context of crack deflection criteria borrowed from models of laminate composites.

The focus of this paper is on the intrinsic mechanical anisotropy of layered perovskites, and

*To whom correspondence should be addressed.
†Current address is Department of Materials, Engineering, III University of California, Santa Barbara, CA 93106, USA.

how it may correlate with a general concept of 'softness'. The anisotropy of the elastic moduli clearly indicates a significantly greater compliance normal to the basal planes than within them. We have interpreted this as weaker bonding between the perovskite blocks based upon analogies with other well known layered compounds such as the micas. This same reasoning can be applied in explaining the anisotropy in fracture toughness, however, the actual mechanisms of fracture are still somewhat vague. 'Softness' in the usual sense of a metal implies that there is a critical number of active slip systems for deformation to occur. This is clearly not the case with layered perovskites where softness is more appropriately attributed to a very low threshold for fracture damage. Layered perovskites have the capacity to bias the direction of crack propagation by virtue of their crystal structure. Although other coincidental mechanisms may also come into play such as micro-fracturing phenomena, it is this latter point that we wish to develop here.

2 Mechanisms of 'softness' and deformation

There have been several examples which illustrate the ease in which layered perovskites like $Na_2Ca_2Nb_4O_{10}$ and $KCa_2Nb_3O_{10}$ can be damaged or can divert cracks at fiber–matrix boundaries.[5] Another demonstration is shown in Fig. 1 which exhibits the fracturing of a ceramic laminate, consisting of a polycrystalline composite of α-Al_2O_3 and K-β-Al_2O_3 as one type of layer (dark phase) and layers of the layered perovskite, $KCa_2Nb_3O_{10}$ (bright phase). The laminate was made by hot pressing stacks of alternating layers of tape cast powders. (The K-β-Al_2O_3, arises from a partial reaction between alumina and $KCa_2Nb_3O_{10}$.) Subsequently, the laminate was fractured in four-point bending, producing the fracture pattern shown. Typically, the crack path is seen to wander within the layered perovskite phase or along the interface between adjacent layers. When a crack penetrates into an alumina layer, it traverses straight across, until it reaches the next $KCa_2Nb_3O_{10}$ layer. Considering that the plate-like grains are preferentially oriented along the prevailing planar orientation of the laminate, this observation further suggests that cracks easily divert along the basal planes of $KCa_2Nb_3O_{10}$.

The 'softness' of layered perovskites is, therefore, likely to be associated with inter-basal cleavage and inter-basal sliding. Electron micrographs of mechanically deformed $KCa_2Nb_3O_{10}$ by Kim *et al.*[6] and of microscopic bubble formation due to excessive intercalation of large chain amines by Treacy *et al.*[7] illustrates the compliant nature of the basal structure and the ease with which the basal planes separate and bend.

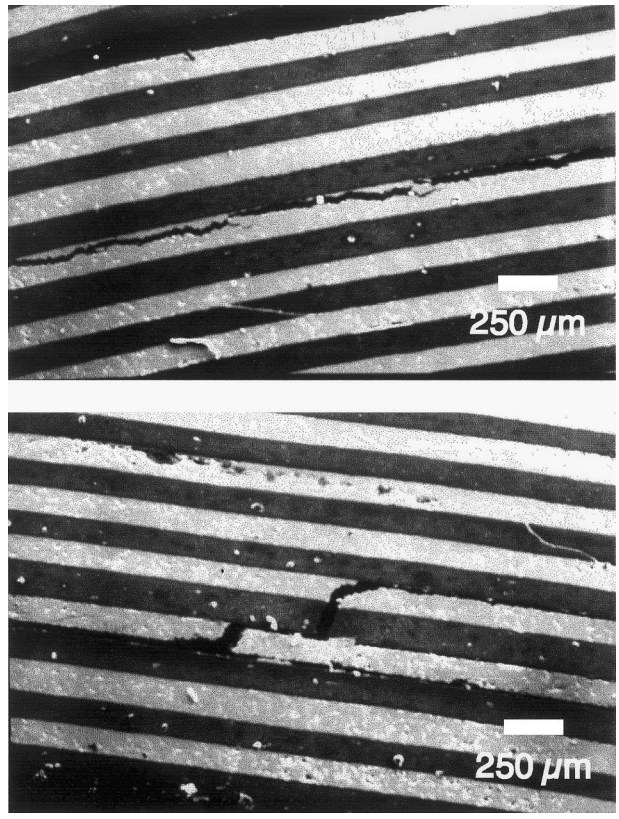

Fig. 1. Back-scattered electron image of the crack paths in a layered composite fractured in four-point bending. The composite consists of layers of $KCa_2Nb_3O_{10}$ (bright phase), alternating with layers of α-Al_2O_3 that contain K-β-Al_2O_3 impurities (dark phase). Arrangement of sample is equivalent to orientation D_{bc} as shown in Fig. 6, except that this material is a composite rather than an anisotropic, homogeneous material. The crack was arranged to run from bottom to top, cutting across the lamellae.

Unlike metals and many ionic solids, which deform by the generation and movement of dislocations, the softness of layered perovskites appears still to be attributable to brittle behavior—but on a microscopic scale. Figure 2 exhibits the fracture damage caused by the drilling of a dimple in a hot pressed pellet of $KCa_2Nb_3O_{10}$. While not measured directly, the load required was quite minor, requiring the same effort as, say, for talc. At higher magnification near the edge of the dimple, Fig. 2(b) shows grains that have split off into flakes that curl and break off into small chips. From this and the evidence of the TEM studies, the severe bending observed of the small flakes indicates a cooperative mechanism of inter basal sliding in order to spatially accommodate the severe strains involved.

3 Structure and anistropy

The common characteristic of layered perovskites as the name suggests, is that the crystal structure

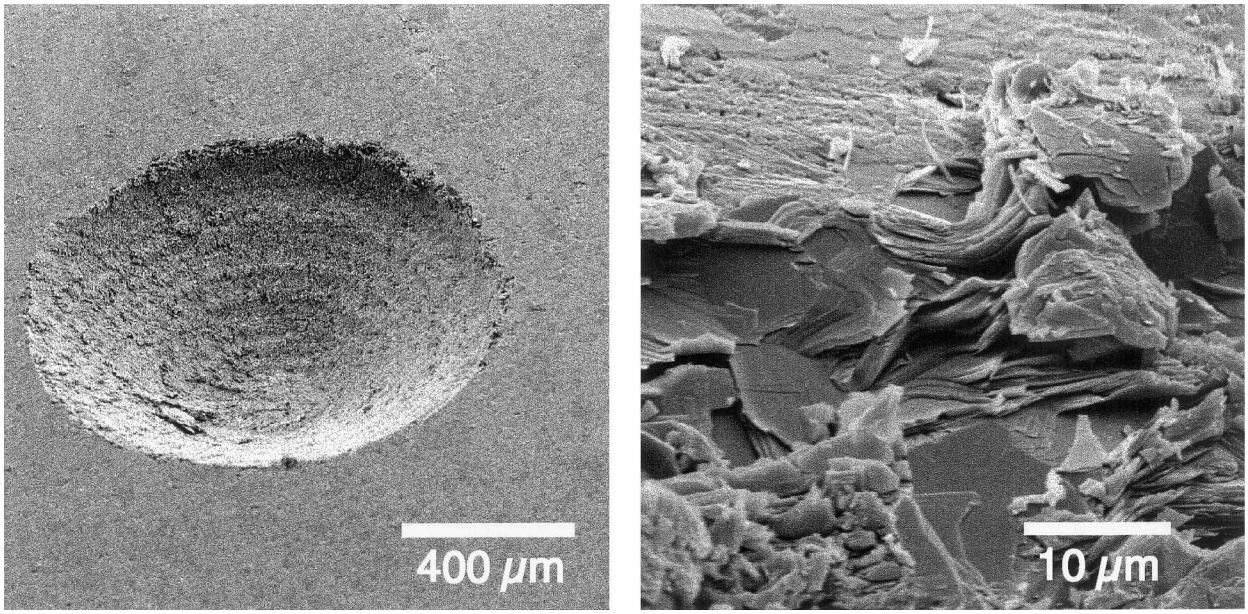

Fig. 2. SEM micrographs of shear damage in sintered $KCa_2Nb_3O_{10}$ produced from a rotary drill. The photograph on the right illustrates damage by delamination, curling and fracturing into small flakes. Some chards illustrate an ability of the material to bend which must be accommodated by cooperative sliding between basal planes.

consists of perovskite blocks bound together by planes of cations, such as for the Dion–Jacobson phases, or by another interleaving crystal structure fragment, such as rock salt $Bi_2O_2^{2+}$ layers in Aurivillius phases.[1,8] Despite this commonality, there is still considerable variety in terms of structure and composition. The thickness of the perovskite blocks can be adjusted with appropriate cation substitutions. This has the affect of adjusting the stiffness of the individual layers. The oxygen coordination about the inter-block cations will differ depending on their ionic size. This affects the details of bond breaking and surface rearrangement when new surfaces form during cleavage.

$KCa_2Nb_3O_{10}$ is included in the class now known as the Dion–Jacobson phases.[9] A schematic of its structure is shown in Fig. 3. It consists of $[Ca_2Nb_3O_{10}]^-$ perovskite blocks separated by individual layers of potassium ions. The perovskite blocks are stacked such that adjacent blocks are translated one-half unit cell distance, $a/2$, relative to one another, thus creating a trigonal prismatic oxygen coordination about the potassium ions. There are twice as many such sites available as there are potassium ions. All of the potassium sites are shown in Fig. 3, although it should be kept in mind that only half will be filled. This disorder in site occupancy may explain the tendencies of $KCa_2Nb_3O_{10}$ of stacking disorder and rapid intercalation kinetics.

Cleavage is most likely along the potassium plane, in analogy with the micas and other sheet silicates. Crack propagation would be more difficult through the perovskite block due to its higher density and bond order than in the vicinity of the potassium layer. While the atom positions for $KCa_2Nb_3O_{10}$ have not been determined precisely, *ab initio* calculations indicate that the potassium sites are arrayed in a corrugated fashion, sitting slightly above and below the average potassium plane.[10] This naturally biases the separation of the potassium ions during cleavage, separating one-half the ions from the other as two new surfaces are created. The low foliation energies calculated indicated an advantage to this bias as compared to other configurations where the interlayer cations are strictly coplanar.

The picture that emerges concerning the soft behavior of layered perovskites is that their high degree of anisotropy plays an important role. It is to be expected that this anisotropy be reflected in many of their physical properties. We have been in the process of determining elastic constants and thermal expansion coefficients as a function of crystallographic direction,[11–13] for the purpose of identifying correlations with fracture anisotropy. While not all of the elastic constants have been determined, critical values are known that can be used to estimate the anisotropy of the fracture energy release.

The Young's moduli and hardnesses of $KCa_2Nb_3O_{10}$ in both the normal and in-plane directions have been determined by nanoindentation experiments.[11] Table 1 summarizes those results and compares them with literature values for other layered structure compounds. Typically, the modulus in the c-direction, $E(\|c)$, is the lowest for each material, reflecting a high compliance due to weaker interatomic bonding between the structural blocks. The moduli reflecting the behavior in

the basal plane, $E(\perp c)$, are higher due in part to the significantly stronger bonding, as in the case for graphite, or greater density of the structural blocks as seen edge-on, such as the perovskite layers. In all cases, there is a substantial anisotropy as indicated by the ratio of moduli. $KCa_2Nb_3O_{10}$ ranks between the sheet silicates and layered spinels typified by Na-β-$A1_2O_3$.

It is useful to examine the elastic behavior of other layered structure compounds where a full complement of elastic compliances are known. Figure 4 presents a polar plot of the longitundinal compliance of graphite and two different micas, i.e., muscovite and phlogopite. These were calculated using the compliances tabulated by Simmons and Wang[14] and the formulas provided by Nye.[15] For comparison, the small, near oval-like feature in the center of the plot corresponds to alumina (corundum structure) which does not possess a layered structure and is structurally almost isotropic.

The longitudinal compliance is defined as the reciprocal of Young's modulus, $1/E$. The vertical axis in Fig. 4 corresponds to the crystallographic c-direction [001] that is normal to the basal planes. The horizontal axis corresponds to any direction in the basal plane.* For a constant stress applied in any direction, the distance from the origin to the curve represents the relative magnitude of strain.

As is expected, there is a relatively large compliance in the c-direction reflecting the weaker bonding between the structural layers. Bonding is

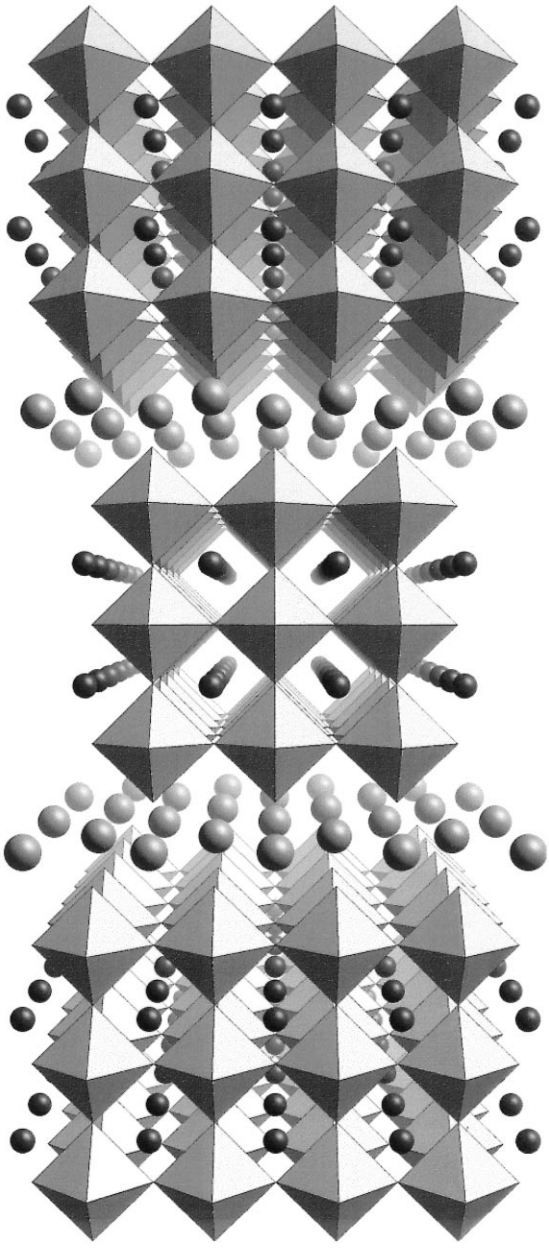

Fig. 3. Schematic of the idealized structure of $KCa_2Nb_3O_{10}$. The corner sharing NbO_6 octahedra establishes the framework of the perovskite layers which are supported by large calcium ions located within 12-fold coordination sites. Potassium is located in trigonal prismatic coordinated sites between the perovskite blocks, arranged in a corrugated fashion.

Table 1. Young's modulus of layered structure compounds

	E(‖c) *GPa*	E(⊥c) *GPa*	$\frac{E(\|c)}{E(\perp c)}$	*Ref.*
Graphite	36	890	0·04	14
Phlogopite	44	135	0·33	14
Muscovite	59	180	0·28	14
$KCa_2Nb_3O_{10}$	57	94	0·61	11
Na-β-Al_2O_3	220	260	0·85	22

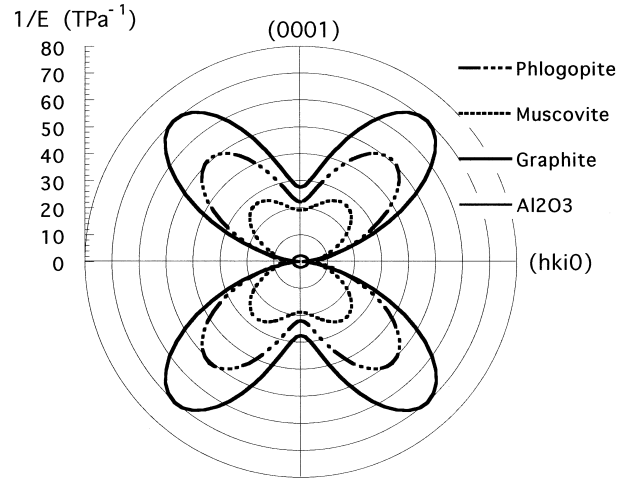

Fig. 4. The longitudinal compliances (inverse Young's modulus, $1/E$) of three layered structure substances are plotted as a function of crystallographic orientation. The vertical axis corresponds to the c-axes which are normal to the basal planes in each case. The horizontal axis lies within the basal plane. The large lobes between axes are due to very large shear compliances.

*The polar plot in Fig. 4 implies orthotropic crystal structures such as might be seen in structures with hexagonal, trigonal and tetragonal symmetries. The c-axis, therefore, represents the long axis which is standard in current crystallographic notation. However, many layered perovskites including $KCa_2Nb_3O_{10}$, possess orthorhombic unit cells or even monoclinic where the b-axis is usually referred to as the long axis. For the sake of clearer comparisons between different layered compounds, we will refer to the long axis as the c-axis, whether it is standard or not.

strong within the basal planes which corresponds to the small compliance plotted along the horizontal axis. Graphite exhibits the extreme difference which reflects the different strengths of van der Waals bonding exerted between graphite sheets and the covalent bonding within the graphite sheets. The surprising feature for all three layered compounds is the large lobes that project roughly between 45 and 54° off the horizontal axis. This corresponds to the contributions from very large shear moduli. The schematic shown in Fig. 5 compares the relative differences in structural distortion due to longitudinal strain in the *c*-axis direction and the much larger shear strain in the off-axis orientation. Drawing an analogy due to the general structural similarities, it is likely that layered perovskites like $KCa_2Nb_3O_{10}$ possess these same sort of characteristics.

4 Experimental

Powders of $KCa_2Nb_3O_{10}$ were prepared by reacting stoichiometric mixtures of $CaCO_3$, Nb_2O_5 and K_2CO_3, to which was added 10% mole excess K_2CO_3 to compensate for volatilization losses. The reaction mixture was heated at 3°C/min to 1250°C and maintained at that temperature for 72 h. The reacted powders were washed repeatedly to remove excess potassium and then dried in air. X-ray diffraction confirmed phase pure $KCa_2Nb_3O_{10}$. The powders were classified, and the −325 mesh component collected for hot pressing.

$KCa_2Nb_3O_{10}$ powders were hot pressed at 1250°C (as determined by optical pyrometry) in 5 cm diameter graphite dies lined with molybdenum foil. The hot press chamber was filled with 0·1 MPa argon to protect the dies from oxidation and to suppress volatilization of potassium. The sample was first heated to the annealing temperature before pressure (14 MPa) was applied. After 0·5 h the sample was cooled under pressure. This procedure produced pellets 5 cm in diameter and 0·5 cm thick and 98% of theoretical density. Their oxide surfaces were slightly reduced evident from a deep blue-purple color. This color quickly disappeared after the pellets were annealed in air at temperatures typically greater than 800°C. The flat surfaces were ground with 600 grit SiC paper to 4 mm thick with less than 0·1 mm variance.

The hot pressed pellets were cut into beams using a diamond wheel saw for single-edge-notched beam (SENB) experiments. Beam sizes were about 4×4 mm in cross-section and about 2·5 cm long. Particular attention was given to the prevailing orientation of the beams relative to the hot pressing direction. A very high degree of preferential crystallographic orientation was observed in the hot pressed pellets as determined by X-ray diffraction. Generally, the crystallographic: long axis (basal normal) of each grain was oriented parallel to the pressing direction. Three types of beams were cut and machined according to the desired orientation of the basal planes. Figure 6 illustrates those orientations with the corresponding designations, D_{2b}, D_{bc} and D_{ca}. The first indice denotes the fracture plane (normal to one of the orthogonal axes a, b or c) and the second refers to the direction of crack propagation.

Because of the limitations of the dimensions of the hot pressed pellets, D_{ca}-oriented beams had to be constructed. The pellet was diced into 4 mm cubes and glued together with cyanoacrylate. The cubes were stacked such that the basal planes of each segment were aligned normal to the beam's long axis. The beams were ground to dimensions consistent with the other previously described beams.

The surfaces of all SENB samples were polished with 800 grit SiC paper. They were notched using a 10 mil (~200 μm) thick diamond wire saw to depths of about 0·25 the thickness of the beam.

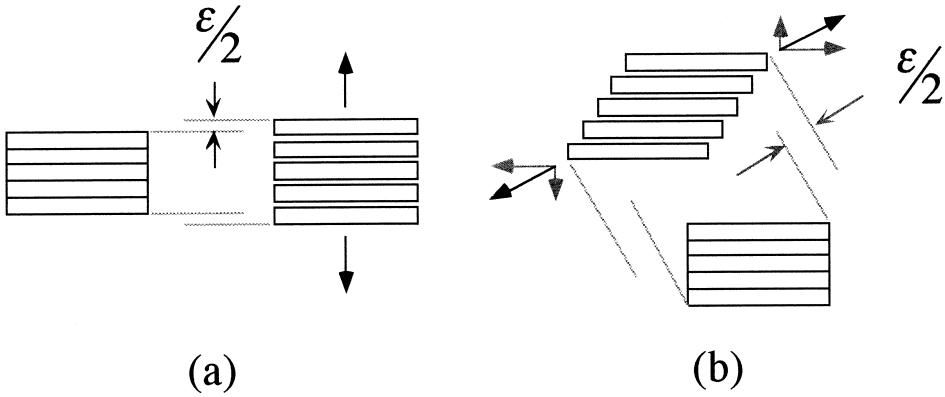

Fig. 5. Schematics illustrating elastic strain in a layered structure compound for the (a) basal normal direction and (b) off-axes directions. The blocks as drawn represent the perovskite layers which are relatively dense and stiff. Interlayer bonding is weak and contributes most to the overall strain. The shear strain is rather large in comparison to normal strains in other crystallographic directions.

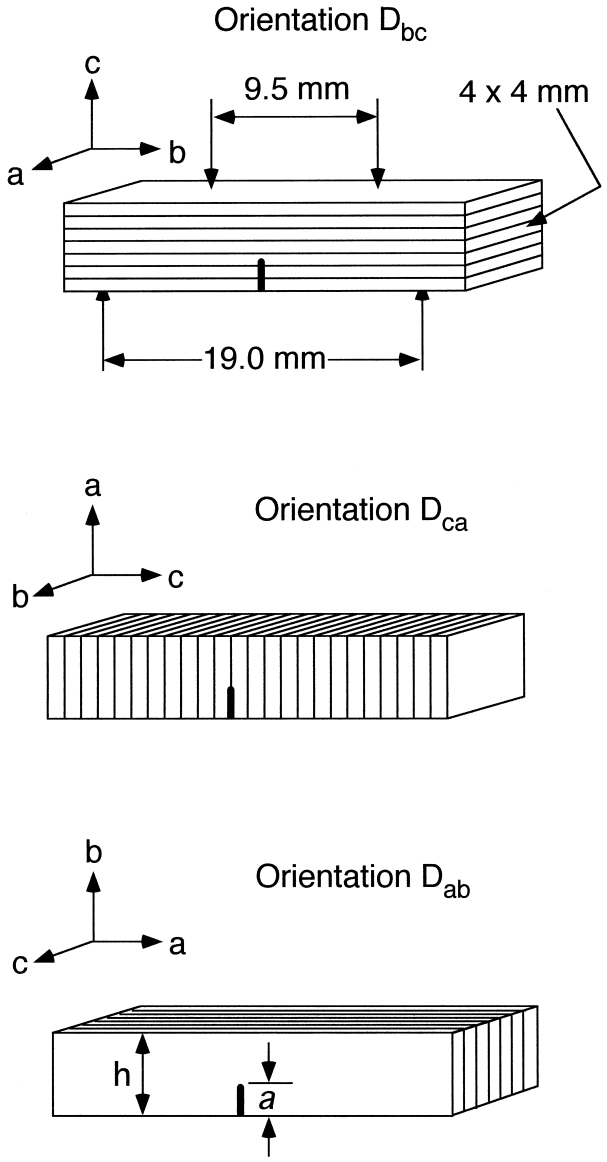

Fig. 6. Configuration of single-edged notch beams used in fracture toughness measurements. Beams were cut from hot pressed disks of $KCa_2Nb_3O_{10}$ which exhibited strong preferential orientation. The three orientations shown correspond to the alignment of the basal planes relative to the fracture plane. The *c*-axis corresponds to the basal normal direction.

Care was taken so that final, residual scratches were aligned along the long beam axis.

Beams specimens were tested in four-point bending using an Instron testing machine interfaced to a personal computer. The bending jig had an outer span of 0·75 in and inner span of 0·375 in. A cross head speed of 1·27 mm/min was used for all tests. The fracture load was recorded directly from the testing machine.

Fracture toughness for SENB specimens was calculated from the maximum load using the expression

$$K_{Ic} = \frac{3PL}{wh^2} a \left[1{\cdot}99 - 2{\cdot}47\left(\frac{a}{h}\right) + 12{\cdot}97\left(\frac{a}{h}\right)^2 - 23{\cdot}17\left(\frac{a}{h}\right)^3 + 24{\cdot}8\left(\frac{a}{h}\right)^4 \right] \quad (1)$$

where P is the maximum load sustained by the specimen, L is the distance between the inner and outer loading points, w and h are the width and height of the test specimen, and a is the notch depth.[16] This equation was derived from elasticity theory and is valid for notched beams tested in four point bending where the relative crack depth is $0{\cdot}1 \leq \frac{a}{h} \leq 0{\cdot}6$. Specimen displacement as a function of time was calculated from the crosshead speed.

5 Results

The high degree of preferential orientation of the hot pressed $KCa_2Nb_3O_{10}$ pellet is illustrated in Fig. 7 which compares the diffraction patterns taken of the top face and cross-section. The (001) reflections are especially dominant in the pattern of the top which are largely suppressed in the pattern of the cross-section. It is evident that the c-axes of each grain are oriented parallel to the hot pressing direction, which is to say that the basal planes themselves are aligned parallel to the faces of the pellet. This texturing is likely due to the plate-like character of the individual powder particles. Experiments on cold pressed powders followed by pressureless sintering exhibited an even higher degree of preferential orientation. This suggests that the small but detectable intensities of (001) reflections in the hot pressed case may be a result of first heating before applying pressure. Nevertheless, the trend is clear with the basal planes of each grain aligning parallel with one another and parallel to the broad, flat faces of the billet.

The scanning electron micrographs shown in Fig. 8 illustrate the texturing of the microstructure. The images shown are of polished and thermally etched surfaces (1250°C, 30 min). The cross-sectional view exhibits the plate-like shape of many of the larger grains with evidence of exaggerated grain growth. A wide range of grain sizes is evident where the largest grain shown is about 90 μm long and 12 μm wide. The smallest grains appear to be in the order of 2–3 μm. The plan view micrograph exhibits more clearly the plate-like nature of the grains where broad areas of smooth basal surfaces are seen. Etch patterns also reveal basal ledges that appear as contours outlining the grains shape. (Curiously, the fine etch patterns seen in the cross-sectional view appear as vertical striations in the large grains. These run 90° to the basal planes which are oriented horizontally in the picture.)

Small pores can be seen in both photographs which accounts for the missing volume in what is 98% dense material (as measured by helium pycnometry). Pores seen in the plan view appear small

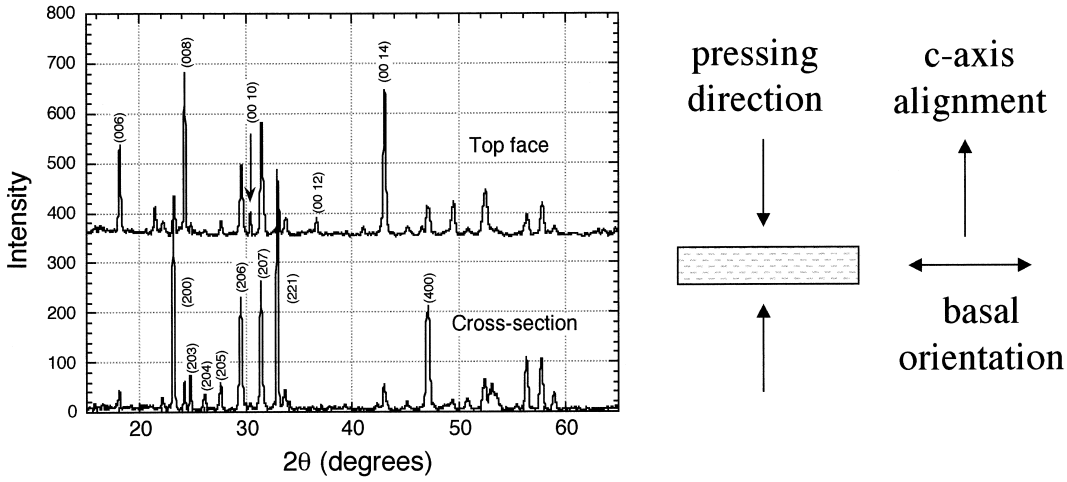

Fig. 7. X-ray diffraction patterns of the top face and cross-section of a hot pressed disks of $KCa_2Nb_3O_{10}$. The strong preferential orientation of the basal planes is indicated by the strong (001) lines in the top pattern. The basal planes are oriented parallel to the flat faces of the disk, normal to the pressing direction.

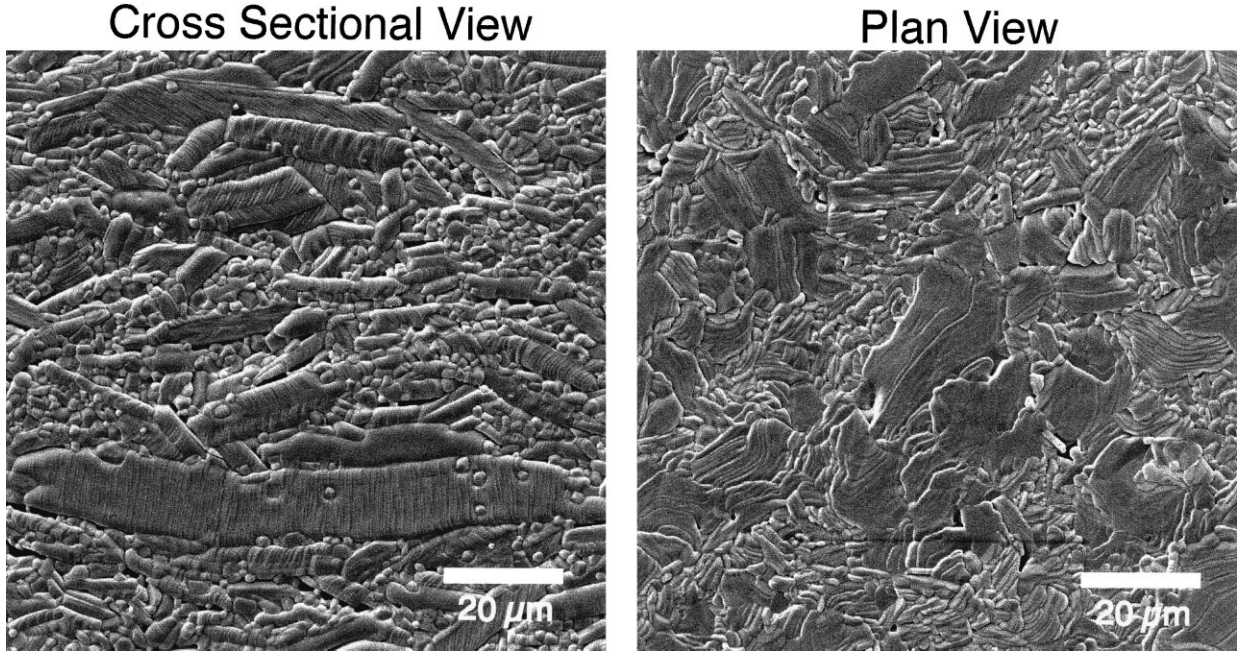

Fig. 8. Scanning electron micrographs of a disk of hot pressed $KCa_2Nb_3O_{10}$. Polished sections of the cross-sectional and plan views were thermally etched at 1250°C for 0·5 h.

and equiaxed relative to the larger grains. In the cross-sectional view, the pores are lenticular in shape and run parallel with the basal orientation.

The results of the single-edged-notch beam tests are given in Table 2 and exhibit the anisotropy expected for $KCa_2Nb_3O_{10}$. Orientation D_{ca} which corresponds to inter basal fracture exhibited the lowest toughness, 0·848 MPa $m^{-\frac{1}{2}}$. The crack travels parallel to the basal planes and is presumed to be severing bonds in the potassium layer whenever a crack is passing through a grain. The fracture toughnesses in the other two orientations are a factor of two or more greater. Fracture in the orientation D_{bc} corresponds to a crack propagating across the perovskite layers (in trans basal fracture mode) and, thus, severs them in sequential fashion. Bonding in the perovskite blocks is stronger due in part to the greater atomic packing and bond order. The fracture toughness in the perpendicular direction, orientation D_{ab}, is even greater. This represents a crack propagating lengthwise through a grain perpendicular to the basal planes such that it cuts through a stack of the perovskite layers at once and splitting them into two-halves. The implication here is that bond breaking is more difficult in this orientation.

There are two experimental issues that affect the precision of the measured fracture toughness. As mentioned previously, the SENB specimens with orientation D_{ca} were constructed by gluing hot pressed cubes together into beams. Of the total six beams fabricated, only two failed properly,

whereby the fracture emanated from the notch. In the other four cases, fracture occurred along or near the glue joints. This means that the fracture toughness stated in Table 2 is based on only two measurements which is less reliable statistically than for the other two orientations, in which there were a total of six measurements each.

The other consideration is that the precut notch for the D_{ca} orientation was not the same in dimensions than for the other two orientations. In particular, the notch was cut with a 0·4 mm thick diamond wheel blade, rather than the 200 μm thick diamond wire saw. Secondly, the notch was cut deeper, being about half the thickness of the beam ($a/h \approx 0{\cdot}5$), whereas the notch was only one-quarter the depth for the other two orientations ($a/h \approx 0{\cdot}25$). Both dimensional differences have the effect of producing observed fracture toughnesses that are greater than what is likely to be intrinsically characteristic of the material. Sakai and Bradt[16] observed that fracture toughness increases with the square root of the crack tip radius if that radius is larger than a critical dimension. Similarly, Simpson[17] indicated that the fracture toughness of many ceramic systems are known to vary with relative notch depth, a/h. As a consequence of applying this analogy, the measured value of the ratio

$$\frac{K_{Ic}(D_{ca})}{K_{Ic}(D_{ab})} \approx 0{\cdot}5 \qquad (2)$$

is likely to be larger than if the experiments were conducted under more consistent conditions. This means that the fracture anisotropy is even larger than is portrayed by the data.

Crack propagation for orientation D_{bc} across the basal planes, yielded characteristically jagged fracture surfaces. While on the one hand, this is responsible for the somewhat greater scatter in the measured values, it is also a reflection, once again, of the anisotropy of this material. Microscopically, the fracture surfaces revealed a zig-zag path for the crack, where the crack apparently advanced in a step-wise fashion of cutting across perovskite layers followed by small lateral diversions along the basal planes. The small lath-like protrusions and depressions in the fracture surface suggest a mechanism where adjacent basal planes act somewhat independently and allow interlayer slip and pull-out.

Table 2. Fracture toughness measured from single-edge notch beam tests

Orientation	K_{Ic} ($MPa\ m^{-1/2}$)
D_{ca} (basal plane)	0·848
D_{bc}	1·615 (±0·142)
D_{ab}	1·863 (±0·072)

6 Discussion

The magnitudes of the fracture toughness of $KCa_2Nb_3O_{10}$ are consistent with cleavage toughness of single crystals of other layered structures. Schultz *et al.*[18] noted that toughness of such crystals as muscovite, graphite, and $YBa_2Cu_3O_7$ are consistently below 1 MPa $m^{-\frac{1}{2}}$, as is the case for the inter basal fracture, D_{ca}, for $KCa_2Nb_3O_{10}$. They also indicated that although the fracture toughness of highly oriented polycrytalline samples of layered compounds are higher than for single crystals of the same general orientation, that the toughness is still low. Highly oriented pyrolytic carbon, for instance, has a cleavage toughness ten times greater than for single crystal graphite, and yet it still is 0·53 MPa $m^{-\frac{1}{2}}$. By analogy, the basal cleavage toughness of single crystal $KCa_2Nb_3O_{10}$ is expected to be significantly smaller than the 0·848 MPa $m^{-\frac{1}{2}}$ reported here for oriented polycrystalline material.

The ability of $KCa_2Nb_3O_{10}$ to bias and redirect the direction of crack propagation can be examined in terms of the relative magnitudes of strain energy release rate, G, for the two predominant directions. For this, we adopt the model of He and Hutchinson[19] that was originally developed for analysing crack deflection criteria in layered and laminated composites of two brittle materials. The fundamental concept borrowed is that crack deflection will occur when the fracture energy release rate in one direction is sufficiently small that it favors diversion of the crack from its current direction which involves a significantly higher fracture energy to propagate. As such, the critical parameter to examine is the ratio of fracture energy release rate in the 'deflected' direction relative to that for the current, or 'penetrating' direction.

The strict application of this model to the current situation is rather coarse. He and Hutchinson's model is based on micron-scale features of a laminated composite, whereas our application is directed at nano-scale dimensions. A layered perovskite is homogeneous, but anisotropic on any scale down to the thickness of the individual perovskite blocks (~12 Å). On the other hand, a laminate composite is anisotropic only on a scale much larger than the individual lamella, whereas within each lamella it is an isotropic substance. Obviously, there will be inconsistencies in the application of crack deflection criteria since the elastic fields about the tip of a crack tip in a layered perovskite will be quite different than in within one component of a

composite. Despite the differences in scale, it is believed that this exercise provides heuristic value which may lead to the development of a more appropriate model.

The schematics in Fig. 9 compare two cracks of different orientations. Crack propagation in the trans basal direction is equivalent to the penetration direction (into adjacent layers) denoted by He and Hutchinson in their model of composites. The second prospect is where a crack travels along the basal direction denoted here as the inter basal splitting mode. In laminated composites, He and Hutchinson refer to this as crack deflection (at the interface between the two layers).

The strain energy release rate is defined as

$$G = \frac{K_{Ic}^2}{E'} \tag{3}$$

where E' is an elastic modulus. For isotropic substances under plane stress conditions, $E'(=E)$ is simply Young's modulus. For orthotropic substances, this modulus is more complex,[20] and involves expressions of several terms of the compliance tensor. The layered perovskite $KCa_2Nb_3O_{10}$ possesses an orthorhombic unit cell which means that a full complement of elastic compliances includes nine independent components. However, only s_{11}, s_{33} and s_{66} are currently known with any degree of assurance. The latter is a shear compliance acting in the basal plane and does not contribute to the current situation. Consequently, with this limitation and for the sake of this discussion, it will be assumed that the effective moduli are equivalent to the Young's moduli given in Table 1. That is, $E'(\| c) = E(\| c)$ for a crack aligned in the basal plane, and $E'(\perp c) = E(\perp c)$ for a crack aligned perpendicularly.

Combining the information from the fracture toughness experiments with the elastic moduli, the strain energy release rate for trans basal crack propagation (penetration mode) is

$$G_p = \frac{[K_{Ic}(D_{bc})]^2}{E(\perp c)} = 27{\cdot}5\,\mathrm{J\,m^{-2}} \tag{4}$$

and for inter-basal crack propagation (deflection mode) is

$$G_d = \frac{[K_{Ic}(D_{ca})]^2}{E(\| c)} = 12{\cdot}6\,\mathrm{J\,m^{-2}} \tag{5}$$

The latter value is particularly interesting in that Chizmeshya *et al.*[10] has calculated the foliation energy for $KCa_2Nb_3O_{10}$ using *ab initio* quantum mechanical methods. That value of $\Gamma_f = 7{\cdot}6\,\mathrm{J\,m^{-2}}$ is equivalent to the energy of cleaving a crystal under uniaxial stress (in vacuo) and thereby creating two new surfaces. There is reasonable agreement between Γ_f and G_d particularly when considering that the theoretical calculation is based on a static model of a single crystal whereas the experimental parameter originates from a dynamic process.

Comparison of the two strain energy release rates simply confirms the pattern that has been observed all along—that is, it is easier for cracks to propogate in the basal plane. The criteria of He and Hutchinson[19] for crack deflection is based on the ratio of the strain energy release rate of the deflected crack over that of a penetrating crack, where

$$\frac{G_d}{G_p} = \left[\frac{K_{Ic}(D_{ca})}{K_{Ic}(D_{bc})}\right]^2 \frac{E(\perp c)}{E(\| c)} \tag{6}$$

A value of 0·45 is calculated for homogeneous $KCa_2Nb_3O_{10}$. Figure 10 places this point in context with the crack deflection criteria for a composite. In the strictest sense, this comparison predicts that no crack deflection should occur since the point lies above the indicated curve. However, the point is not too far off especially when considering the experimental limitations of the results already discussed. It is to be expected that this fracture toughness ratio in eqn (6) for $KCa_2Nb_3O_{10}$ will be smaller when more accurate and complete data are available. In addition, the ratio of the elastic moduli may also decrease when more components of the elastic tensor are measured and can be included in the calculation.

It is worth noting that several studies on ceramic composite systems have shown that crack deflection occurred even though the strain energy release rate ratio was significantly greater than predicted by the criteria of He and Hutchinson.[19] Crack deflection clearly occurs in individual grains of $KCa_2Nb_3O_{10}$. It is believed that the He and Hutchinson model contains the general features needed to examine crack deflection in severely anisotrophic solids.

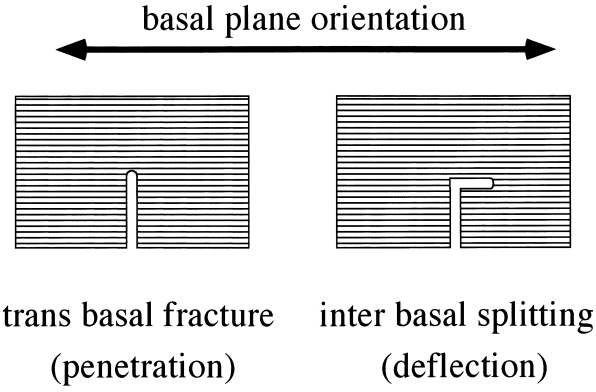

Fig. 9. Orientation of crack propagation relative to the crystallographic basal planes. Corresponding fracture energy release rates were calculated for each orientation and used in a discussion on crack deflection criteria similar to a model developed by He and Hutchinson for layered composites.[19]

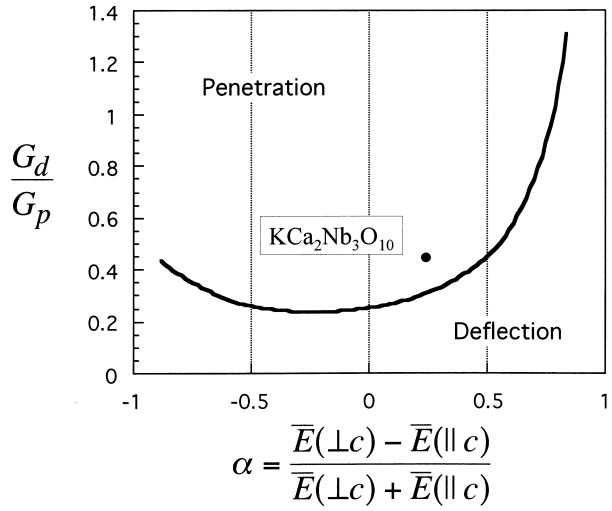

Fig. 10. The ratio of the fracture energy release rates as a function of the relative difference in the Young's modulus for parallel and perpendicular to the crystallographic *c*-axis. The *c*-axis coincides with the basal normal. The curve is the criteria established by He and Hutchinson[19] for layered composites, whereas the point is for the homogeneous, but anisotropic layered perovskite $KCa_2Nb_3O_{10}$.

Such a model must take into account the nature of the anisotropy which is that of a homogeneous solid, rather than the condition imposed by an interface between two different isotropic substances.

7 Conclusions

The large mechanical anisotropy of the the layered perovskite $KCa_2Nb_3O_{10}$ is considered to be a key feature related to the ease in which this compound can be damaged. Anisotropy in the elastic moduli and fracture toughness both reflect the relatively weak interlayer bonding between perovskite layers in the structure. The extension of this to anisotropy in fracture energy release rate suggests that the 'softness' of this compound can be explained in terms of the ability for cracks to be deflected and other processes such as the microfracturing of the perovskite layers.

$KCa_2Nb_3O_{10}$ represents a general class of layered perovskites which has great variety in composition and structural details. This presents the opportunity to adjust the physical properties to suit certain design goals. Demonstrations of the friability and damage absorption suggest that these materials may find utility in ceramic-matrix-composites and other applications where a combination of 'softness', thermal stability and oxidation resistance is desired.

Acknowledgements

The authors wish to thank Drs T. A. Parthasarathy, M. Cinibulk and R. J. Kerans (all of the Materials and Manufacturing Directorate, Air Force Research Laboratories, Wright-Patterson AFB), and Professor R. C. Bradt (University of Alabama) for their generous discussions elucidating various aspects of fracture mechanics. Usage of the hot pressing and mechanical testing facilities at Wright-Patterson Air Force Base are also greatly appreciated. Funding from the US Air Force Office of Sponsored Research under award F49620-95-1-0155 is gratefully acknowledged.

References

1. Jacobson, A. J., Synthesis and reaction chemistry of layered oxides with perovskite related structures. In *Chemical Physics of Intercalation II, NATO ASI Series*, 305, ed. P. Bernier *et al.* Plenum Press, Chateau de Bonas, France, 1993, pp. 117–139.
2. Mohan Ram, R. A. and Clearfield, A., Synthesis and intercalation chemistry of $K[Ca_2(Ca,Sr)_{n-3}Ti_{n-3}O_{3n+1}]$ (n = 4, 5). *J. Solid State Chem.*, 1991, **94**, 45–51.
3. Jacobson, A. J., Johnson, J. W. and Lewandowski, J. T., Interlayer chemistry between thick transition metal oxide layers: synthesis and intercalation reactions of $K[Ca_2Na_{n-3}Nb_nO_{3n+1}]$ ($3 \leq n \leq 7$). *Inorg. Chem.*, 1985, **24**, 3729–3733.
4. Takano, Y., Takayanagi, S., Ogawa, S., Yamadaya, T. and Mori, N., Superconducting properties of layered perovksites $KCa_2Nb_3O_{10}$ and $KLaNb_2O_7$. *Sol. State Comm.*, 1997, **103**(41), 215–217.
5. Petuskey, W. T. and Sambasivan, S., Layered perovskites as boundary phases in ceramic–matrix-composites. *J. Mat. Res.* (submitted).
6. Kim, S. T., Dravid, V. P. and Sambasivan, S., Chemical and morphological analysis of sol-derived $KCa_2Nb_3O_{10}$. *J Mat. Res.*, 1999, **14**, 1327–1328.
7. Treacy, M. M., Rice, S. B., Jacobson, A. J. and Lewandowski, J. T., Electron microscopy study of delamination in dispersions of perovskite related layered phases $K[Ca_2Na_{n-3}Nb_nO_{3n+1}]$; evidence for single-layer formation. *Chem Mater.*, 1990, **2**, 279–286.
8. Frit, B. and Mercurio, J. P., The crystal chemistry and dielectric properties of the Aurivillius family of complex bismuth oxides with perovskite-like layered structures. *J. Alloy and Compounds*, 1992, **188**, 27–35.
9. Uma, S. A., Raju, R. and Gopalakrishnan, J., Bridging the Ruddlesden–Popper and the Dion–Jacobson series of layered perovskites: synthesis of layered oxides, $A_{2-x}La_2Ti_{3-x}Nb_xO_{10}$ (A = K,Rb), exhibiting ion exchange. *J. Mater. Chem.*, 1993, **3**(7), 709–713.
10. Chizmeshya, A. V. G. and Petuskey, W. T., Thermoelastic propeties of layered perovskites: a non-empirical density functional theory approach. In *High Temperature Ceramics: Experiment and Theory*, eds. A. Pechenik, P. Vashishta and Kalia R. Oxford University Press, Oxford, 1999, pp. 504–518.
11. Shemkunas, M. P. and Petuskey, W. T., Nanoindentation of a layered crystal structure oxide. In *Fundamentals of Nanoindentation and Nanotribology*, ed. N. R Moody, W. W Berberich, N. Burnham and S. P Baker. Materials Research Society Symposium Proceedings, 1998, Vol. 522, pp 275–280.
12. Steiner, K. A., Thermal expansion and compressibility of layered perovskite compounds. M.S. Thesis, Arizona State University, Tempe, AZ, 1998.
13. Steiner, K. A. and Petuskey, W. T., High pressure synchrotron diffraction of $KCa_2Nb_3O_{10}$, a layered perovskite compound. In *Application of Synchrotron Radiation Techniques to Materials Science*, ed. S. M. Mini, S. R.

Stock, D. L. Perry and L. J. Terminello. Materials Research Society Symposium Proceedings, 1998, Vol. 524, pp 133–137.
14. Simmons, G. and Wang, H., *Single Crystal Elastic Constants and Calculated Aggregate Properties: A Handbook*, 2nd edn., MIT Press, Cambridge, Massachusetts, 1971.
15. Nye, J. F., *Physical Properties of Crystals*, Oxford University Press, Oxford, 1972, pp. 143–145.
16. Sakai, M. and Bradt, R. C., Fracture toughness testing of brittle materials. *International Materials Reviews*, 1993, **38**(21), 53–78.
17. Simpson, L. A., Use of the notched-beam test for evaluation of fracture energies of ceramics. *J. Am. Ceram. Soc*., 1974, **57**(41), 151–154.
18. Schultz, R. A., Jensen, M. C. and Bradt, R. C., Single crystal cleavage of brittle materials. *Int. J. Fract*., 1994, **65**, 291–312.
19. He, M. and Hutchinson, J. W., Crack deflection at an interface between dissimilar elastic materials. *Int. J. Solids Structures*, 1989, **25**(9), 1053–1067.
20. Sih, G. C., Paris, P. C. and Irwin, G. R., On cracks in rectilinearly anisotropic bodies. *Int. J. Fract. Mech*., 1965, **1**, 189.
21. Lee, W., Howard, S. J. and Clegg, W. J., Growth of interface defects and its effect on crack deflection and toughening criteria. *Acta Met*., 1996, **44**(10), 3905–3922.
22. McWhan, D. B., Shapiro, S. M., Remeika, J. P. and Shirane, G., Neutron-scattering studies on beta-alumina. *J. Phys. C. Solid State Phys*., 1975, **8**, L487–L491.